Report

Current Biology

Grapefruit-derived nootkatone potentiates GABAergic signaling and acts as a dual-action mosquito repellent and insecticide

Graphical abstract

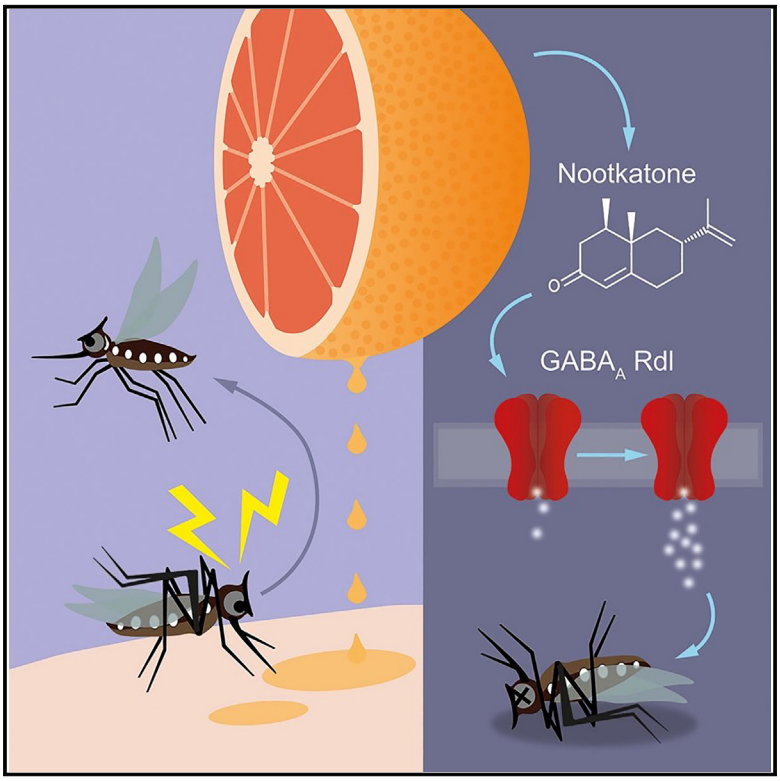

Highlights

- Nootkatone, found in grapefruit, acts as both a repellent and an insecticide
- Spatial aversion in *Aedes aegypti* involves Orco and ionotropic receptor neurons
- The proboscis senses nootkatone for contact repellency, independent of TRPA1 and IRs
- Nootkatone modulates Rdl channels, potentiating GABA inhibition in mosquitoes

Authors

Merybeth Fernandez Triana, Felipe Andreazza, Nadia Melo, ..., Christopher J. Potter, Ke Dong, Marcus C. Stensmyr

Correspondence

marcus.stensmyr@biol.lu.se

In brief

Triana and Andreazza et al. describe nootkatone, a grapefruit volatile, as a potent mosquito repellent and an insecticide. Nootkatone induces spatial and contact repellency, preventing feeding, and potentiates GABA-mediated inhibition, causing paralysis. Its safety for humans and pleasant scent makes nootkatone a promising option for mosquito control.

Fernandez Triana et al., 2025, Current Biology *35*, 177–186
January 6, 2025
https://doi.org/10.1016/j.cub.2024.10.067

CellPress

Current Biology

CellPress
OPEN ACCESS

Report

Grapefruit-derived nootkatone potentiates GABAergic signaling and acts as a dual-action mosquito repellent and insecticide

Merybeth Fernandez Triana,[1,2,7] Felipe Andreazza,[3,7] Nadia Melo,[1] Rickard Ignell,[2,4] Ali Afify,[5,6] Yuan Li,[3] Dan-Dan Zhang,[1] Christopher J. Potter,[5] Ke Dong,[3] and Marcus C. Stensmyr[1,2,8,*]

[1]Department of Biology, Lund University, Lund 22362, Sweden
[2]Max Planck Center next Generation Chemical Ecology, Lund 22362, Sweden
[3]Department of Biology, Duke University, Durham, NC 27708, USA
[4]Disease Vector Group, Department of Plant Protection Biology, Swedish University of Agricultural Sciences, Lomma 23422, Sweden
[5]The Solomon H. Snyder Department of Neuroscience, Johns Hopkins University School of Medicine, Baltimore, MD 21205, USA
[6]Department of Biology, Drexel University, Philadelphia, PA 19104, USA
[7]These authors contributed equally
[8]Lead contact
*Correspondence: marcus.stensmyr@biol.lu.se
https://doi.org/10.1016/j.cub.2024.10.067

SUMMARY

Humanity has long battled mosquitoes and the diseases they transmit—a struggle intensified by climate change and globalization, which have expanded mosquito ranges and the spread of associated diseases.[1] Additionally, widespread insecticide resistance has reduced the efficacy of current control methods, necessitating new solutions.[2,3] Nootkatone, a natural compound found in grapefruit, shows promise as both a mosquito repellent and an insecticide.[4,5] However, its mechanism of action remains unclear. Our study demonstrates that nootkatone acts as a potent spatial and contact repellent against multiple mosquito species. Nootkatone-induced spatial aversion, which is influenced by human odor, is in *Aedes aegypti* partially mediated by Orco- and ionotropic receptor (IR)-positive neurons, while contact aversion is robust and likely mediated via the proboscis and independent of TRPA1 and IRs. We further find that nootkatone potentiates γ-aminobutyric acid (GABA)-mediated signaling by modulating the broadly expressed major insect GABA-gated chloride channel resistant to dieldrin (Rdl). At low doses, the chemosensory-mediated spatial and contact repellency is likely strengthened by nootkatone's disruption of synaptic transmission in select mosquito sensory neurons. At higher doses, nootkatone induces paralysis and death, presumably through broad-range synaptic transmission disruption. These findings reveal nootkatone's unique mode of action and highlight its potential as an effective mosquito control agent. Its dual role as a repellent and an insecticide, combined with low-to-no toxicity to humans and a pleasant smell, underscores nootkatone's promise as a future tool in mosquito control efforts.

RESULTS AND DISCUSSION

Nootkatone spatially displaces mosquitoes but not when human scent is present

In the 1600s, the Caribbean was a bustling hub of commerce and colonization. In this melee of galleons coming and going—intermixed with swashbuckling adventures and buccaneering on the high seas—many new commodities were introduced to the region.

One such commodity was the pomelo (*Citrus grandis*). The widely accepted story suggests that seeds of this fruit were brought to Barbados in the mid-1600s by a certain Captain Phillip Chaddock (Figure 1A), a British trader sailing under charter from King Charles II (1630–1685) and possibly associated with the *Honorable Company of Adventurers for the Somers Islands*.[6] The pomelo quickly hybridized with Chinese sweet oranges (*Citrus sinensis*) present on the island, with the pomelo serving as maternal parent and sweet orange providing pollen.[6] The resulting offspring (back then known as the forbidden fruit) was much praised for its distinct tangy taste and quickly spread across the Caribbean. Today, this apomictically stabilized hybrid is known as grapefruit (*Citrus* × *paradisi*), and is a staple on many breakfast tables.

Grapefruit has inherited many characteristics from its maternal parent, including its size, color, thick peel, pulp texture, and tartness, as well as the biosynthetic pathway for nootkatone.[7] This sesquiterpene (Figure 1B) has a distinct and pleasant smell to the human nose and is widely used as a flavoring and fragrance agent in food and hygiene products to mimic the scent of grapefruit. To some arthropods, however, nootkatone is not pleasant but induces strong aversion and, at high doses, paralysis and ultimately death.[4,8,9]

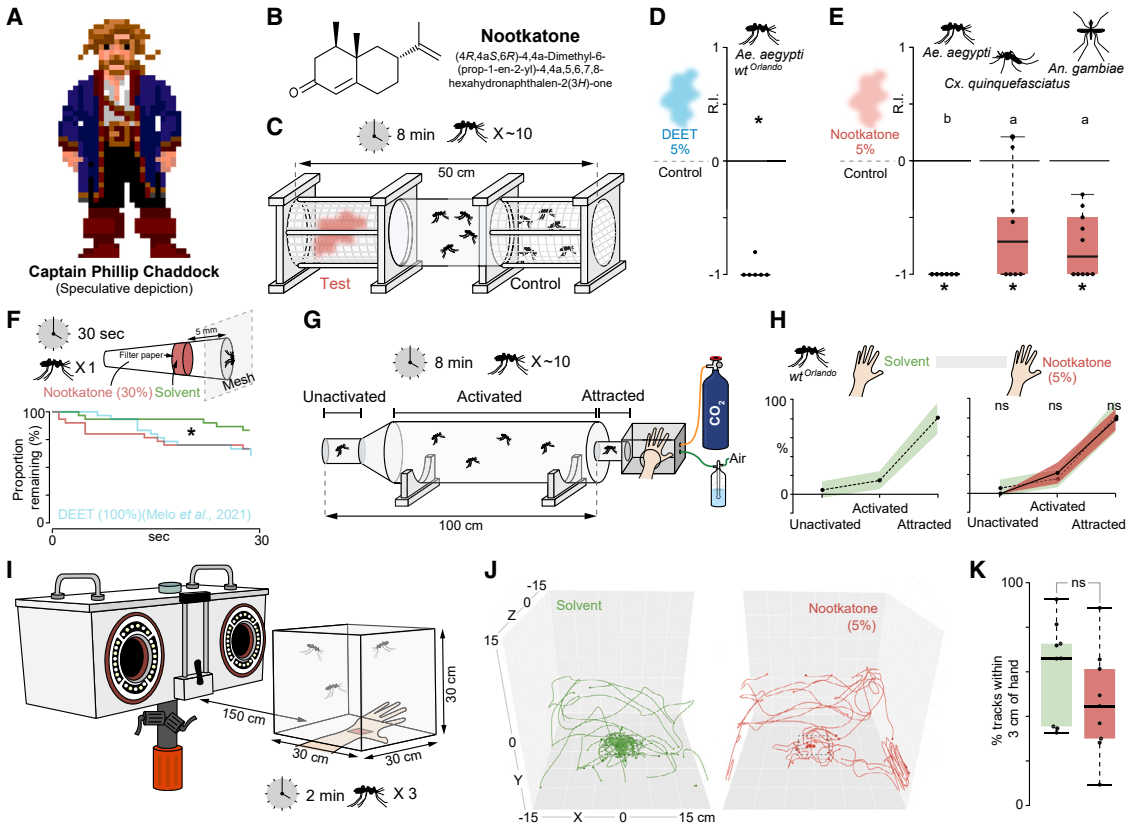

Figure 1. Nootkatone is a spatial repellent

(A) Speculative depiction of Captain Phillip Chaddock, British merchant and credited with having brought pomelo seeds to Barbados in the 1600s.

(B) The chemical structure of nootkatone and its full systematic IUPAC name.

(C) Schematic drawing of the standard WHO spatial repellency assay.

(D and E) Repellency indices (RIs) from wild-type (WT) *Ae. aegypti* confronted with 5% w/v DEET (D) and WT *Ae. aegypti*, *Culex quinquefasciatus*, and *An. gambiae* confronted with 5% w/v nootkatone (E) in the WHO spatial repellency assay (10 mosquitoes/trial; $n = 6–10$). RI = $(Nc - Nt)/(Nc + Nt)$, where Nc = number of females in the control chamber and Nt = number of females in the treatment chamber. The edges of the boxes are the first and third quartiles, while the thick lines inside the boxes indicate the medians. Whiskers represent the data range. Preference was evaluated using a one-sample Wilcoxon signed-rank test against a theoretical mean of 0. Black star denotes a significant difference from 0 ($p < 0.05$). Differences between groups were analyzed using the Mann-Whitney U test. Similar letter denotes no significant difference ($p > 0.05$).

(F) Kaplan-Meier estimates showing the proportions of *Ae. aegypti* remaining on the cage wall over time in response to 30% w/v nootkatone, acetone and DEET ($n = 30$ mosquitoes). Differences between groups were analyzed using the Cox proportional hazard model. Black star indicates significant differences from control ($p < 0.05$).

(G) Schematic drawing of the uniport olfactometer assay.

(H) WT *Ae. aegypti* (10 mosquitoes/trial; $n = 5–10$) freely orienting in a CO_2-spiked airstream toward a human hand treated with either solvent or 5% w/v nootkatone. The shaded area indicates the standard deviation. Differences between control and treatment were analyzed using the Mann-Whitney U test. "ns" denotes no significant difference ($p > 0.05$).

(I) Schematic drawing of the photonic fence monitoring device (PFMD).

(J) Example PFMD generated tracks from WT *Ae. aegypti*, exposed to a patch of human skin (denoted by a dashed line) coated with either solvent or 5% w/v nootkatone.

(K) Percentage of tracks within 3 cm of the exposed skin (3 mosquitoes/trial; $n = 9$). Boxplots as per (D and E). Statistical difference was assessed using a paired samples Student's t test. ns denotes no significant difference ($p > 0.05$).

See also Table S1.

Studies over the past 2 decades, spearheaded by the Centers for Disease Control and Prevention (CDC), have demonstrated that nootkatone is effective in warding off arthropods, including mosquitoes.[5,9–11] In 2020, the US Environmental Protection Agency (EPA) approved nootkatone for use as a repellent and biopesticide (EPA Pesticide Chemical [PC] Code: 030806), opening the path for widespread application of this compound.

Nootkatone possesses several appealing qualities when compared with N,N-diethyl-3-methylbenzamide (DEET)—the present gold standard among insect repellents. It is a natural compound, does not degrade plastic, is non-greasy, has a nice smell, and is even safe for consumption.[12] As a result, once nootkatone-based repellents become available, they are likely to quickly gain popularity. Although evidently effective, precisely how nootkatone works remains unknown.

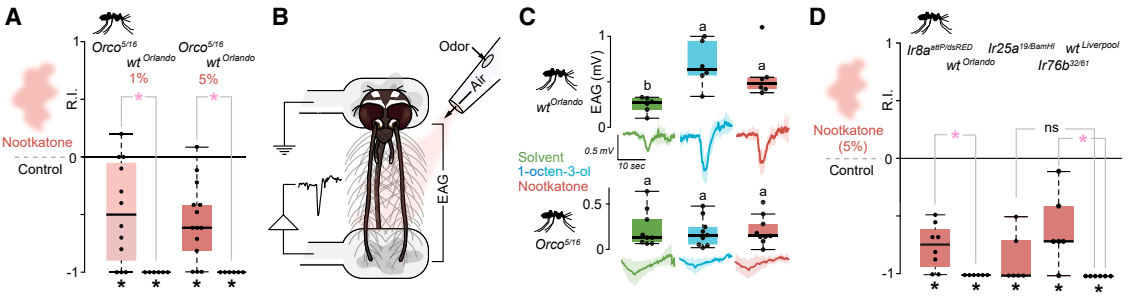

Figure 2. Molecular components mediating nootkatone's spatial aversion

(A) RIs from *Orco*$^{5/16}$ and the WT (Orlando strain) *Ae. aegypti* genetic background control exposed to nootkatone (either 1% w/v or 5% w/v) (10 mosquitoes/trial; n = 6–12). RI = ($Nc - Nt$)/($Nc + Nt$), where Nc = number of females in the control chamber and Nt = number of females in the treatment chamber. The edges of the boxes are the first and third quartiles, while the thick lines inside the boxes indicate the medians. Whiskers represent data range. Preference was evaluated using one-sample Wilcoxon signed-rank test against a theoretical mean of 0. Black star denotes a significant difference from 0 ($p < 0.05$). Difference against genetic background strain was examined via Kruskal-Wallis test. Pink star denotes a significant difference from background ($p < 0.05$).

(B) Schematic drawing of the electroantennography (EAG) preparation.

(C) EAGs from WT (Orlando) and *Orco*$^{5/16}$ *Ae. aegypti*; n = 6–9. EAG traces shown are averages of multiple traces, with shaded areas representing the standard deviation. Boxplots as per (A). Differences between groups were analyzed using the Mann-Whitney U test. Similar letter denotes no significant difference ($p > 0.05$).

(D) RIs from IR co-receptor mutant *Ae. aegypti* strains exposed to 5% w/v nootkatone (10 mosquitoes/trial; n = 6–8). Boxplots and statistics as per (A).

See also Table S1.

To begin unraveling the function of nootkatone, we first used the standardized World Health Organization (WHO) spatial repellency assay[13] (Figure 1C), which prevents direct contact between mosquitoes and the test substance. As a positive control, we screened DEET (5%), which exhibited clear spatial repellency in *Aedes aegypti* females (Figure 1D). Nootkatone at 5% was equally effective, with none of the *Ae. aegypti* remaining in the treated chamber (Figure 1E). We also tested the Southern house mosquito (*Culex quinquefasciatus*) and the African malaria mosquito (*Anopheles gambiae*) in the same assay, both of which were also repelled by nootkatone, although slightly less so than *Ae. aegypti* (Figure 1E). Repellency of *Ae. aegypti* to nootkatone was also observed in a close proximity response assay[14] (Figure 1F), where nootkatone (at a high dose of 30%) showed a repellency level comparable with what we previously found for DEET (100%) in this assay.[15]

To assess whether nootkatone retains its effectiveness in repelling mosquitoes in the presence of human scent, we conducted a uniport olfactometer assay[16] (Figure 1G) to monitor the behavior of female *Ae. aegypti* flying upwind toward a human hand treated with nootkatone or solvent. An exposed hand treated with solvent triggered robust upwind flight (Figure 1H). Application of 5% nootkatone did not affect the mosquitoes' behavior (Figure 1H), nor did increasing the concentration to 10% (data not shown). To investigate if nootkatone inhibits spatial attraction at close range when human scent is present, we used a photonic fence monitoring device (PFMD), capable of automatically tracking multiple flying mosquitoes (Figure 1I). We introduced female *Ae. aegypti* into a cage, allowing them to approach a patch of human skin in the bottom, but preventing direct contact. Skin treated with solvent attracted the mosquitoes (Figure 1J), with the mosquitoes staying close (here defined as 3 cm) to the skin surface (Figure 1K). Treatment with 5% nootkatone had little effect on the behavior of the mosquitoes (Figure 1J). Although the mosquitoes showed a tendency to spend less time close to the skin when nootkatone was present (Figure 1K), this difference did not reach statistical significance.

Together, these results show that volatile nootkatone confers spatial repellency in mosquitoes, which is largely neutralized by the simultaneous presence of sensory cues emitted from human skin.

Spatial repellency is partially OR and IR mediated

How does nootkatone mediate spatial repellency? We investigated nootkatone aversion in *Ae. aegypti* lacking Orco, a co-receptor necessary for the proper function of ligand-selective odorant receptors (ORs).[17,18] The *Orco*$^{5/16}$ mutants exposed to 1% or 5% nootkatone in the WHO repellency assay retained similar aversion, with no significant difference (Student's t test: $t(21) = 2.08$, $p = 0.74$) (Figure 2A), although to a lesser extent than the genetic background (*Orlando*), in which these concentrations caused complete spatial displacement (Figure 2A).

To verify that *Ae. aegypti* detects nootkatone via *Orco*-positive neurons, we examined antennal responses using electroantennography (EAG) (Figure 2B). EAG responses to nootkatone were stronger than those to the solvent and comparable to those elicited for 1-octen-3-ol, a compound emitted from human skin[19] (Figure 2C). These responses were abolished in *Orco*$^{5/16}$ mosquitoes (Figure 2C). In summary, while *Orco*-positive neurons detect nootkatone and contribute to spatial repellency, they do not seem to be the sole pathway for aversion in *Ae. aegypti* because mosquitoes lacking *Orco* still exhibit repellency.

In mosquitoes, as in other insects, volatile compounds are also detected by ionotropic receptors (IRs).[16,20,21] Could the IR pathways contribute to the spatial repellency of nootkatone? Similar to ORs, the IR family relies on co-receptors (Ir8a, Ir25a, and Ir76b) for the proper functioning of the ligand-selective IRs.[21–23] We tested *Ae. aegypti* mutant strains lacking each of these IR co-receptors[16,20] with 5% nootkatone. Although all three mutant strains were still repelled by nootkatone, both *Ir76b*$^{32/61}$ and *Ir8*$^{attP/dsRED}$ showed significantly reduced aversion compared

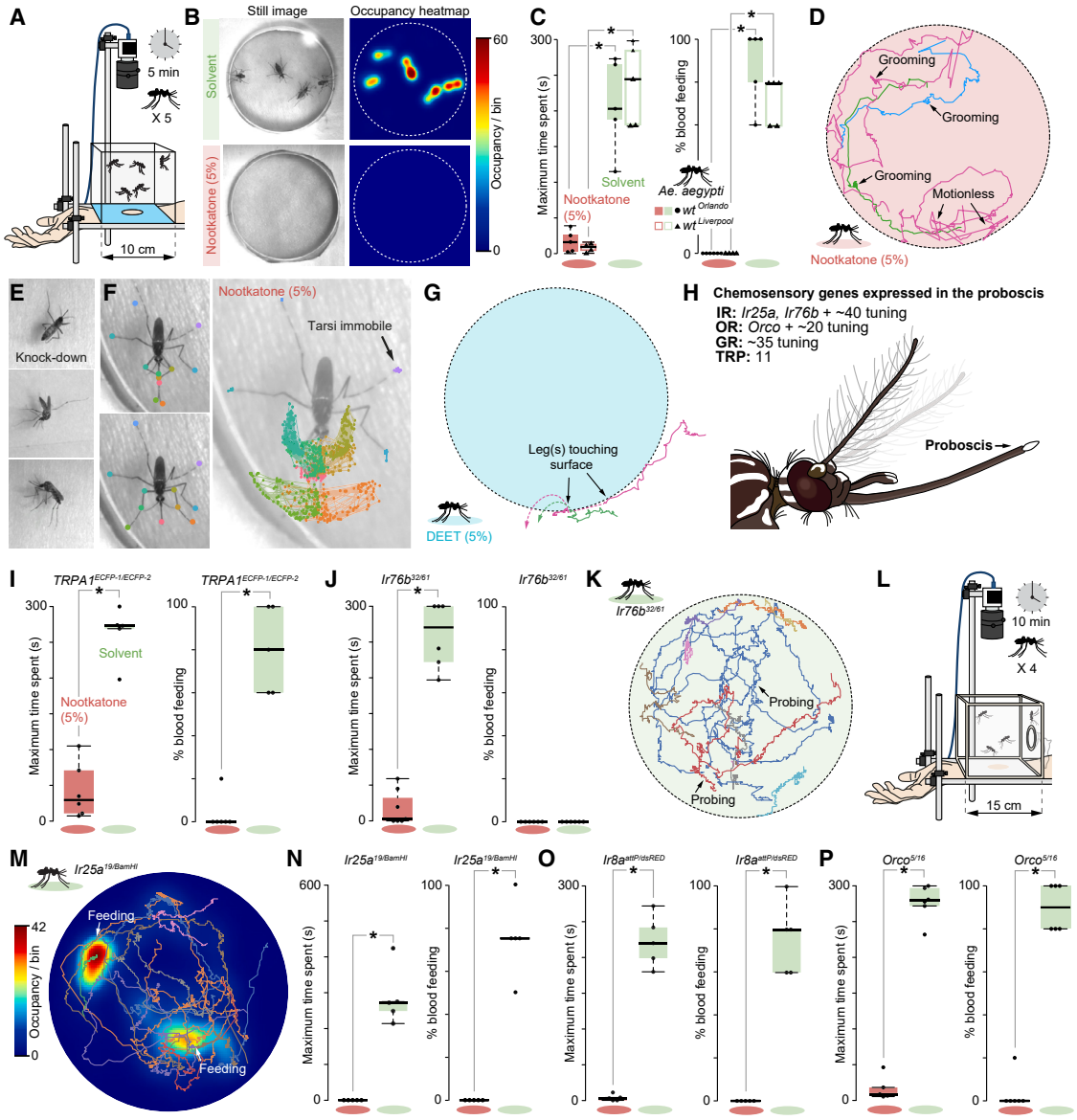

Figure 3. Nootkatone contact aversion is independent of IRs and TRPA1

(A) Schematic drawing of the close-up feeding assay.

(B) Example still image (left) and heatmap (right, based on occupancy/bin) from a single experiment showing the positions of WT *Ae. aegypti* (Orlando strain) over 5 min on the surface of human skin treated with either solvent or 5% w/v nootkatone.

(C) Average of maximum time spent by WT *Ae. aegypti* (Orlando and Liverpool strain) on the surface of skin treated with either 5% w/v nootkatone or solvent in the close-up feeding assay (left) and (right) the percentage of these mosquitoes proceeding to blood feed from skin treated with nootkatone or solvent in the same assay (5 mosquitoes/trial; $n = 4–6$). The edges of the boxes are the first and third quartiles, while the thick lines inside the boxes indicate the medians. Whiskers represent data range. Statistical differences were examined using the Kruskal-Wallis test. Black star denotes a significant difference between nootkatone and solvent treatments ($p < 0.05$).

(D) Superimposed tracks from individual WT *Ae. aegypti* (Orlando strain) navigating across human skin treated with nootkatone 5% w/v.

(E) Paralyzed WT *Ae. aegypti* on nootkatone-treated skin.

(F) Tracks of individual body parts of a WT *Ae. aegypti* exposed to 5% w/v nootkatone vigorously grooming its proboscis.

(G) Superimposed tracks from a single WT *Ae. aegypti* (Orlando strain) navigating in the vicinity of human skin treated with 5% w/v DEET.

(H) Chemosensory appendages of *Ae. aegypti* and the chemosensory genes expressed in the proboscis.[30]

(I) Maximum time spent by *TRPA1*$^{ECFP-1/ECFP-2}$ *Ae. aegypti* on the surface of skin treated with either 5% w/v nootkatone or solvent in the close-up feeding assay (left) and (right) the percentage of these mosquitoes proceeding to blood feed from skin treated with nootkatone or solvent in the same assay (5 mosquitoes/trial; $n = 5–6$). Boxplots and statistics as per (C).

(legend continued on next page)

with the genetic background (Liverpool and Orlando, respectively) (Figure 2D).

Full loss of spatial aversion may require the simultaneous disruption of separate Orco-, and IR co-receptor-dependent pathways, with each contributing to the overall aversion. Alternatively, repellency could be mediated by neurons that co-express these co-receptors. Recent studies in both *Drosophila melanogaster*[22] and *Ae. aegypti*[23,24] have demonstrated widespread co-expression of chemosensory co-receptors in olfactory sensory neurons. One such interesting non-canonical neuron class in *Aedes* expresses OR14 and OR15, along with all co-receptors. Notably, OR15 responds to a broad range of structurally dissimilar plant-derived repellents[25,26] and may also be responsive to nootkatone. Parts of the aversion could also be non-chemosensory mediated and stem from the neurotoxicity of nootkatone.[4,5] Pyrethrin and derived pyrethroid insecticides confer Orco-independent spatial repellency through hyperactivation of voltage-gated sodium channels.[27,28] It is conceivable that a similar mechanism might be at work here as well.

Nootkatone is an effective contact repellent

While conferring spatial repellency is an advantageous trait of nootkatone, from an epidemiological standpoint, inhibiting arthropod disease vectors from engaging in blood feeding is clearly more important.

To examine whether nootkatone also has contact repellency properties, we used a "close-up feeding assay" (Figure 3A). Mosquitoes were confined within a Plexiglas enclosure and tracked in 2D using the multi-animal pose tracking software, Social LEAP Estimates Animal Pose (SLEAP).[29] Heatmaps generated from mosquito thorax positions over a 5-min tracking period showed that, with application of a 5% nootkatone solution, none of the mosquitoes spent extended periods on the surface (Figures 3B and 3C), and none proceeded to blood feed (Figure 3C). Heatmaps from skin treated with solvent showed mosquitoes spending extended periods on the surface and engaged in blood feeding (Figures 3B and 3C).

Interestingly, after landing, mosquitoes did not immediately take off; instead, they were observed scurrying across the nootkatone-treated surface (Figure 3D). On average, mosquitoes stayed on the skin for 6.14 ± 1.38 s (avg ± SEM; $n = 49$ landing events, Orlando and Liverpool pooled), during which they touched the skin with their proboscis 1.30 ± 0.39 times before evacuating and sometimes becoming immobilized (Figure 3E). The feeding attempts were promptly aborted and typically followed by vigorous grooming of the proboscis (but not the antennae) (Figure 3F). Of note, the tracked mosquito in Figure 3F is standing on nootkatone-coated skin, and although the front legs are repeatedly moved along the proboscis, the middle and posterior legs remain immobile on the nootkatone-coated surface. In short, the mosquitoes appear untroubled by having their tarsi in prolonged contact with nootkatone but reluctant to touch the surface with their proboscis beyond the first attempt. This behavior is in stark contrast to that triggered by DEET, where brief tarsal contact induces rapid takeoff,[31,32] which we also observed in our close-up feeding assay (Figure 3G). Taken together, these experiments suggest that contact aversion is primarily mediated via the proboscis, a notion that will need to be confirmed via electrophysiology or functional imaging.

Nootkatone contact aversion is independent of IRs and TRPA1

Chemoreceptors expressed in the proboscis include ORs, IRs, gustatory receptors (GRs), and transient receptor potential (TRP) channels[30] (Figure 3H). The latter family includes the nociceptor *TRPA1*, which is activated by heat and noxious compounds.[33,34] *TRPA1* is also a known target of natural insect repellents, including citronellal[35] and nepetalactone,[15] and could accordingly also be responsible for detecting nootkatone. $TRPA1^{ECFP\text{-}1/ECFP\text{-}2}$ mutants[34] displayed a slight loss of aversion in the close-up feeding assay (Figure 3I); however, this difference was not statistically significant compared with the behavior of the genetic background Liverpool strain(ANOVA test [$F(1,8) = 2.95$, $p = 0.12$]).

The IR co-receptor *Ir76b* is expressed at high levels in the proboscis.[30] Although its primary function appears to be detection of volatile amines,[36,37] it could in theory also function in contact chemosensation. The $Ir76b^{32/61}$ mutants (Figure 3J), however, displayed no abnormal contact aversion toward nootkatone compared with Liverpool strain (ANOVA test [$F(1,9) = 0.51$, $p = 0.49$]). The $Ir76b^{32/61}$ mosquitoes also did not feed from nootkatone-treated skin. Curiously, however, neither did these mutants feed from solvent treated skin (Figure 3J). The mosquitoes could be seen vigorously probing the skin surface (Figure 3K) but never proceeded to complete a blood meal. The failure of the $Ir76b^{32/61}$ mosquitoes to blood feed is an intriguing phenotype that merits further investigation. Feeding phenotype aside, these experiments do show that these mutants have no reduced contact aversion toward nootkatone.

Ir25a is the most highly expressed chemosensory gene in the proboscis[30] and is involved in chemo-, taste, thermo-, and hygrosensation.[38–42] In *D. melanogaster*, Ir25a is expressed in neurons signaling aversive taste[43] and therefore a prime candidate to operate in potential nootkatone-sensing gustatory neurons. However, in the close-up feeding assay, the $Ir25a^{19/BamHI}$ mutants were uncooperative, with none of the mosquitoes

(J) Maximum time spent by $Ir76b^{32/61}$ *Ae. aegypti* on the surface of skin treated with either 5% w/v nootkatone or solvent in the close-up feeding assay (left) and (right) the percentage of these mosquitoes proceeding to blood feed from skin treated with nootkatone or solvent in the same assay (5 mosquitoes/trial; $n = 6–7$). Boxplots and statistics as per (C).
(K) Tracks from individual $Ir76b^{32/61}$ *Ae. aegypti* navigating across human skin treated with solvent.
(L) Schematic drawing of the modified close-range feeding assay.
(M) Tracks from individual $Ir25a^{19/BamH1}$ *Ae. aegypti* navigating across human skin treated with solvent, plotted on top of a heatmap (based on occupancy/bin) showing the mosquitoes' position over 5 min.
(N–P) Maximum time spent by *Ae. aegypti* chemosensory mutant strains ($Ir25a^{19/BamH1}$, $Ir8a^{attp/dsRE}$, and $Orco^{5/16}$) on the surface of skin treated with either 5% w/v nootkatone or solvent in the close-up feeding assay (left in each subpanel) and (right) the percentage of these mosquitoes proceeding to blood feed from skin treated with nootkatone or solvent in the same assay (5 mosquitoes/trial; $n = 5–6$). Boxplots and statistics as per (C).

approaching the exposed skin (even after 20 min of observation). Replacing the Plexiglass box in the assay with a mesh cage (Figure 3L) made the mosquitoes more active, and although they never fully engorged, they eventually engaged in blood feeding (Figure 3M). Application of nootkatone abolished any prolonged contact with the skin and blood-feeding attempts in the *Ir25a*$^{19/BamHI}$ mutants (Figure 3N). In short, the contact aversion is not mediated by *Ir25a*-dependent pathways.

We also examined mutants for the co-receptors *Ir8a* and *Orco* and their associated tuning receptors.[30] Mutants for these two co-receptors examined in the close-up assay (using the original assay configuration) displayed no reduced aversion toward nootkatone (Figures 3O and 3P) compared with the Orlando strain (ANOVA test [$F(1,8) = 1.71$, $p = 0.23$ and $F(1,8) = 0.003$, $p = 0.96$, respectively]).

The contact aversion may be mediated through GRs expressed in the proboscis. Of the ~35 GRs expressed in this structure,[44] several have orthologs in *D. melanogaster* that confer bitter taste and avoidance behavior. Another possibility is that nootkatone activates the nociceptive TRP channel Painless,[45] which is also strongly expressed in the proboscis,[30] and responsive to aversive compounds.[46] A third possibility is that nootkatone does not activate chemoreceptors but that contact avoidance—as well as spatial repellency—is wholly or partially mediated through some other mechanism(s).

Nootkatone potentiates GABA-mediated inhibition

In the close-up feeding assay, mosquitoes showed distinct symptoms consistent with a neurotoxic effect of nootkatone (Figure 3F). To verify its insecticidal activity, we used the WHO susceptibility assay, a standardized test used to assess the effectiveness of insecticides in adult mosquitoes (Figure 4A).[47] *Ae. aegypti* exposed to nootkatone were quickly affected, with nootkatone not only causing temporal paralysis (knockdown) but also mortality, with roughly half the mosquitoes exposed to 20% nootkatone ending up dead after 24 h and about a quarter if 10% was used (Figure 4A).

Our findings of nootkatone evoking spatial and contact repellency at low to moderate doses and knockdown and mortality at high doses are reminiscent of the actions of transfluthrin, a volatile pyrethroid insecticide. Transfluthrin activates voltage-gated sodium (Na_v) channels, causing neuronal hyperactivity and paralysis at high doses and Orco-independent spatial repellency at nonlethal doses.[27] Therefore, we examined the possible effects of nootkatone on an *Ae. aegypti* sodium channel ($AaNa_v1$-1) expressed in *Xenopus* oocytes under two-electrode voltage clamp (TEVC) (Figure 4B). However, unlike transfluthrin, nootkatone did not alter $AaNa_v1$-1 channel gating nor did it block sodium currents (Figures 4C, 4D, S1A, and S1B). These results indicate that nootkatone does not act on sodium channels.

A study in *Drosophila* larvae using whole-cell patch clamp recordings of central neurons reported a reduction in γ-aminobutyric acid (GABA) inhibition when nootkatone was applied.[48] Additionally, nootkatone's toxicity also differed between a cyclodiene-resistant and a susceptible *Drosophila* strain.[48] These findings contrast with mortality data from *An. gambiae*, in which no difference in lethal dosage of nootkatone was observed between a cyclodiene-resistant and a susceptible strain.[49]

To determine whether nootkatone inhibits or potentiates GABA action, we next examined the effect on the *Ae. aegypti* GABA-gated chloride channel Rdl (resistant to dieldrin) expressed in *Xenopus* oocytes. Rdl is a broadly expressed major $GABA_A$ receptor in insects and was initially isolated from *D. melanogaster* strains resistant to dieldrin, an insecticide that specifically targets GABA-gated chloride channels.[50] Dieldrin (and related insecticides such as lindane and fipronil) cause neurotoxicity by blocking Rdl channels, thereby disrupting inhibitory neurotransmission.

We isolated a full-length Rdl clone—*AaRdl1-1*—from *Ae. aegypti*, which we functionally expressed in *Xenopus* oocytes. Using TEVC, we examined the *AaRdl1-1* channel's response to GABA, both in the absence or presence of nootkatone. GABA-induced currents were detected from oocytes injected with the *AaRdl1-1* cRNA, which were fully blocked by 100 nM of fipronil confirming that *AaRdl1-1* is, indeed, an *Rdl* GABA receptor (Figure S1C).

The application of GABA rendered stable peak current amplitudes within the first test pulses. Having established GABA activation, we next, in a stepwise manner, increased the GABA concentration pulsed onto the oocyte, which resulted in a stepwise increased current amplitude response that plateaued at 1,000 μM GABA (Figure 4E). The same oocyte was then pulsed with saline before testing it with 100 μM nootkatone, which did not reveal agonist-like action on AaRdl1-1 (Figure 4E). We then added 100 μM nootkatone to the bath flow to maintain its constant presence throughout the recording and generated another GABA-concentration-response curve (Figures 4E and 4F). Nootkatone increased the responsiveness of AaRdl1-1 to GABA, causing a 4.8-fold leftward shift of the response curve and a significantly smaller GABA EC_{50} than in the absence of nootkatone.

We next set to test the dose-response effect of nootkatone in a fixed GABA concentration background of 100 μM. After obtaining a stable current amplitude response for 100 μM GABA in the absence of nootkatone (Figure 4G), we proceeded to increase the nootkatone concentration until a near-maximum plateau was reached at 100 μM (Figure 4H). The nootkatone effect was dose dependent, and using the last GABA pulse for each nootkatone concentration as the maximum effect for each concentration, we found that nootkatone induced a maximum 4.5-fold increase at 100 μM (Figure S1D).

In summary, these experiments demonstrate that nootkatone potentiates GABA-mediated inhibition. Nootkatone accordingly works differently from other insecticides, such as dieldrin, lindane, and fipronil, which also operate on the same molecular target but similar to the monoterpenoid thymol—the key aroma compound of garden thyme (*Thymus vulgaris*)—which also acts as a positive allosteric $GABA_A$ receptor modulator.[51] Similar to pyrethrins, nootkatone's repellency could also, in part, stem from modification of synaptic transmission, and while pyrethrins cause hyperactivation of nervous signaling, nootkatone causes increased inhibition of synaptic transmission.

Conclusions

We demonstrate that nootkatone is an effective mosquito repellent. Spatial aversion, which is modulated by human odor, is partially mediated by Orco and IR positive neurons, while contact aversion is mediated via the proboscis and is independent

CellPress
OPEN ACCESS

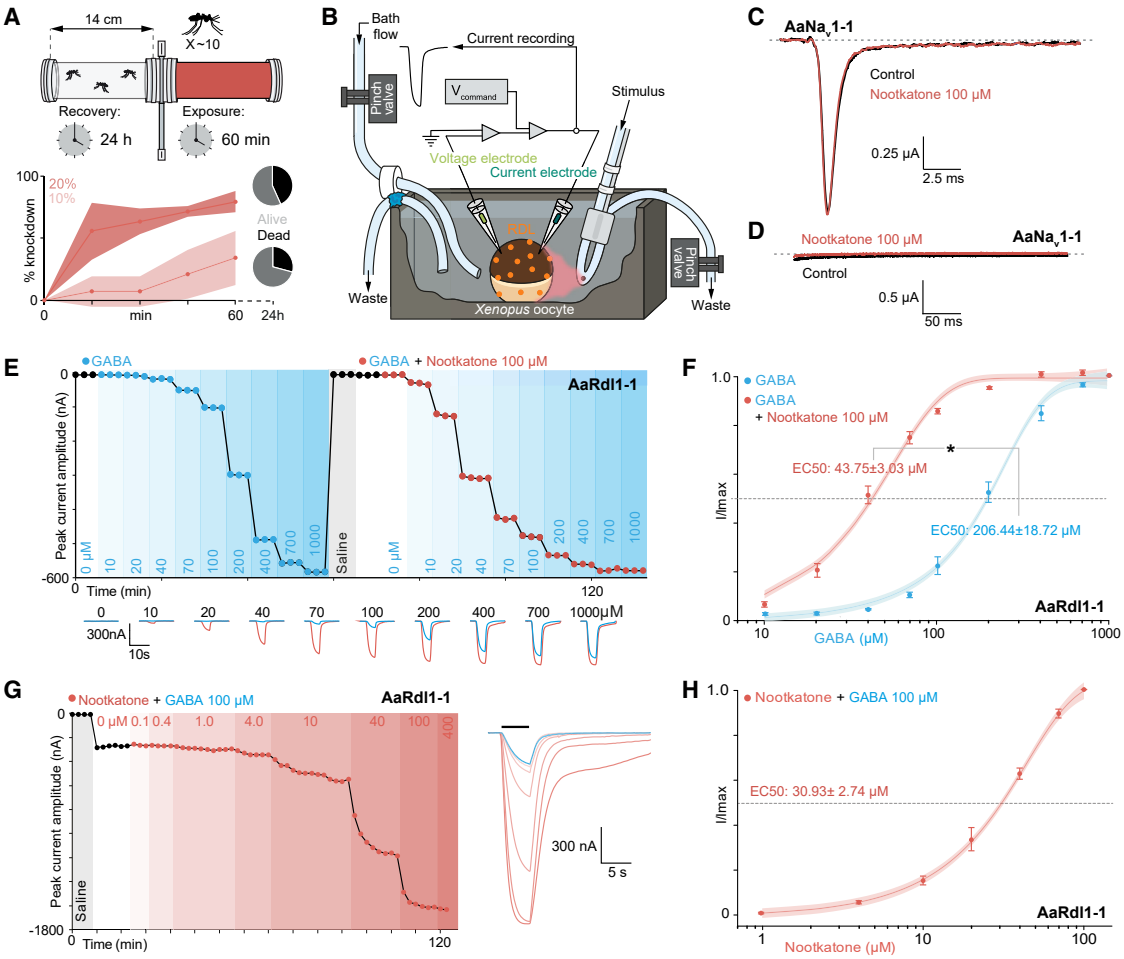

Figure 4. Nootkatone potentiates GABA-mediated inhibition

(A) Schematic drawing of the WHO susceptibility assay (top). Proportion of knockdown WT *Ae. aegypti* exposed to nootkatone (10% or 20% w/v) over time (bottom). The shaded area indicates standard deviation (10 mosquitoes/trial; $n = 4$).

(B) Schematic drawing of the two-electrode voltage clamp setup.

(C) Representative trace of the typical transient inward sodium current upon step membrane depolarization from −120 to 10 mV, with nearly complete inactivation of the AaNa$_v$1-1 channel after a few ms.

(D) Representative traces showing absence of the typical tail current induced by pyrethroids after repolarization to −120 mV from a −10 mV test pulse after 100 × 66 Hz 5 ms pre-pulses to −10 mV.

(E) Time course example of GABA concentration responses on AaRdl1-1 expressed in one oocyte in the absence (blue dots, from 0 to 58 min) or presence (grapefruit-colored dots, from 60 to 132 min) of nootkatone 100 μM, with overlaid current traces from the last pulse at each concentration (bottom).

(F) Concentration-response curves for GABA in the presence or absence of 100 μM nootkatone. Normalized GABA-induced currents (blue and grapefruit-colored dots) were fitted with Boltzmann function (continuous line). Error bars represent the mean ± SEM, and the shaded area indicates the 95% confidence interval of the fitted curve ($n = 5$). Difference between EC_{50} values was tested with a Student's t test ($p < 0.001$).

(G) Time course example of nootkatone concentration responses on AaRdl1-1 expressed in one oocyte stimulated with GABA 100 μM (left), with overlaid current traces from the last pulse at each concentration (right).

(H) Concentration-response curve for nootkatone + GABA (100 μM). Normalized GABA + nootkatone-induced currents were fitted with Boltzmann function (continuous line). Error bars represent the mean ± SEM, and the shaded area indicates the 95% confidence interval of the fitted curve ($n = 5$).

See also Figure S1.

of TRPA1 and IRs. Nootkatone potentiates GABA-mediated inhibition through positive allosteric modulation of the GABA-gated chloride channel Rdl. At low doses, the chemosensory-mediated spatial and contact repellency is likely strengthened by nootkatone's disruption of synaptic transmission in select mosquito sensory neurons. At higher doses, nootkatone induces paralysis and death, presumably through disrupting broad-range synaptic transmission.

Further studies are required to evaluate the underlying neuronal mechanisms of nootkatone-activated Rdl involvement in both toxicity and repellency, as well as to identify the neuronal population in the proboscis conferring contact aversion. The Rdl channel is broadly, but not uniformly, expressed in the insect nervous system, and in *Ae. aegypti*, it is most highly expressed in the brain.[30] Small lipophilic molecules, such as nootkatone, can easily dissolve in the lipid-rich epicuticle, facilitating their

passage into the insect's body and nervous system. Exposure to volatile nootkatone is sufficient to induce paralysis. The different *in vivo* effects of nootkatone at low versus high doses could result from the potentiation of different Rdl variants. Indeed, insect Rdl genes undergo extensive alternative splicing and RNA editing, generating Rdl variants with different sensitivities to GABA and/or insecticides.[52–55] At sublethal low doses, nootkatone might potentiate only a subset of Rdl variants that are more sensitive to it, thereby enhancing the chemosensory-mediated component of the repellent effect. Prolonged exposure to high concentrations of nootkatone would induce broad-range potentiation of GABA-mediated inhibitory transmission, leading to paralysis, as observed.

The effectiveness of nootkatone as both a repellent and an insecticide, combined with its low-to-no toxicity for humans and pleasant smell, makes this compound a promising future mosquito control agent.

RESOURCE AVAILABILITY

Lead contact

Further information and requests for resources and reagents should be directed to and will be fulfilled by the lead contact, Marcus C. Stensmyr (marcus.stensmyr@biol.lu.se).

Materials availability

This study did not generate new unique reagents.

Data and code availability

All data reported in this paper will be shared by the lead contact upon request. This paper does not report original code. Coding sequence for the AaRdl1-1 is deposited in GenBank with accession code: PQ497334. Any additional information required to reanalyze the data reported in this paper is available from the lead contact upon request.

ACKNOWLEDGMENTS

We thank Titus Farkas, Esther Evans, and Sophia Friedrich for assisting with behavioral experiments and mosquito rearing. Special thanks to Matthew DeGennaro and Leslie B. Vosshall for providing mosquito strains. We thank Evolva AG (now part of Danstar Ferment AG) for kindly providing nootkatone. We thank Global Health Labs, Inc and Photonic Sentry Labs for the kind donation of the Photonic Fence Monitoring Device. M.C.S., M.F.T., D.-D.Z., and R.I. were supported by the Max Planck Center for Next Generation Chemical Ecology, while K.D. and F.A. received funding from the NIH (GM057440). N.M. acknowledges support from Formas (2019-01590). C.J.P. and A.A. were supported by grants from the NIH (NIAID R01AI137078) and the Department of Defense (W81XWH-18-1-0732).

AUTHOR CONTRIBUTIONS

M.F.T. and M.C.S. conceptualized the study, with data curation by M.F.T. and F.A. Formal analysis and visualization were carried out by M.F.T., F.A., and M.C.S. Funding acquisition and resources were provided by M.C.S., R.I., C.J.P., and K.D. The investigation and methodology were performed by M.F.T., F.A., N.M., A.A., Y.L, and D.-D.Z., while M.C.S. managed the project. The original draft was written by M.F.T., F.A., K.D., and M.C.S., with all authors contributing to the review and editing.

DECLARATION OF INTERESTS

The authors declare no competing interests.

STAR★METHODS

Detailed methods are provided in the online version of this paper and include the following:

- KEY RESOURCES TABLE
- EXPERIMENTAL MODEL AND STUDY PARTICIPANT DETAILS
  - Animal rearing
- METHOD DETAILS
  - Chemical reagents
  - Mosquito behavior experiments
  - Electroantennography (EAG)
  - Isolation of an *Aedes aegypti* Rdl full-length cDNA
  - Expression of *AaegRdl1-1* and *AaNa$_v$1-1* in *Xenopus* oocytes
  - Two-electrode voltage clamp recordings and data analysis
- QUANTIFCATION AND STATISTICAL ANALYSIS

SUPPLEMENTAL INFORMATION

Supplemental information can be found online at https://doi.org/10.1016/j.cub.2024.10.067.

Received: September 3, 2024
Revised: October 23, 2024
Accepted: October 28, 2024
Published: December 3, 2024

REFERENCES

1. Ryan, S.J., Carlson, C.J., Mordecai, E.A., and Johnson, L.R. (2019). Global expansion and redistribution of *Aedes*-borne virus transmission risk with climate change. PLoS Negl. Trop. Dis. *13*, e0007213. https://doi.org/10.1371/journal.pntd.0007213.
2. Siddiqui, J.A., Fan, R., Naz, H., Bamisile, B.S., Hafeez, M., Ghani, M.I., Wei, Y., Xu, Y., and Chen, X. (2022). Insights into insecticide-resistance mechanisms in invasive species: Challenges and control strategies. Front. Physiol. *13*, 1112278. https://doi.org/10.3389/fphys.2022.1112278.
3. Chaudhry, A., Jabeen, R., Sarfraz, B., and Mazhar, S. (2019). Mosquito control methods and their limitations. Pure Appl. Biol. *8*, 2389–2398. https://doi.org/10.19045/bspab.2019.80184.
4. Panella, N.A., Dolan, M.C., Karchesy, J.J., Xiong, Y., Peralta-Cruz, J., Khasawneh, M., Montenieri, J.A., and Maupin, G.O. (2005). Use of novel compounds for pest control: insecticidal and acaricidal activity of essential oil components from heartwood of Alaska yellow cedar. J. Med. Entomol. *42*, 352–358. https://doi.org/10.1093/jmedent/42.3.352.
5. Clarkson, T.C., Janich, A.J., Sanchez-Vargas, I., Markle, E.D., Gray, M., Foster, J.R., Black, W.C., Foy, B.D., and Olson, K.E. (2021). Nootkatone is an effective repellent against *Aedes aegypti* and *Aedes albopictus*. Insects *12*, 386. https://doi.org/10.3390/insects12050386.
6. Kumamoto, J., Scora, R.W., Lawton, H.W., and Clerx, W.A. (1987). Mystery of the forbidden fruit: Historical epilogue on the origin of the grapefruit, *Citrus paradisi* (Rutaceae). Econ. Bot. *41*, 97–107. https://doi.org/10.1007/BF02859356.
7. MacLeod, W.D., Jr., and Buigues, N.M. (1964). Sesquiterpenes. I. Nootkatone, a new grapefruit flavor constituent. J. Food Sci. *29*, 565–568. https://doi.org/10.1111/j.1365-2621.1964.tb00411.x.
8. Handore, K.L., Kalmode, H.P., Sayyad, S., Seetharamsingh, B., Gathalkar, G., Padole, S., Pawar, P.V., Joseph, M., Sen, A., and Reddy, D.S. (2019). Insect-repellent and mosquitocidal effects of noreremophilane-and nardoaristolone-based compounds. ACS Omega *4*, 2188–2195. https://doi.org/10.1021/acsomega.8b03652.
9. Zhu, B.C., Henderson, G., Chen, F., Maistrello, L., and Laine, R.A. (2001). Nootkatone is a repellent for Formosan subterranean termite (*Coptotermes formosanus*). J. Chem. Ecol. *27*, 523–531. https://doi.org/10.1023/a:1010301308649.

10. Dietrich, G., Dolan, M.C., Peralta-Cruz, J., Schmidt, J., Piesman, J., Eisen, R.J., and Karchesy, J.J. (2006). Repellent activity of fractioned compounds from *Chamaecyparis nootkatensis* essential oil against nymphal Ixodes scapularis (Acari: Ixodidae). J. Med. Entomol. *43*, 957–961. https://doi.org/10.1603/0022-2585(2006)43[957:raofcf]2.0.co;2.

11. Dolan, M.C., Jordan, R.A., Schulze, T.L., Schulze, C.J., Manning, M.C., Ruffolo, D., Schmidt, J.P., Piesman, J., and Karchesy, J.J. (2009). Ability of two natural products, nootkatone and carvacrol, to suppress *Ixodes scapularis* and *Amblyomma americanum* (Acari: Ixodidae) in a lyme disease endemic area of new jersey. J. Econ. Entomol. *102*, 2316–2324. https://doi.org/10.1603/029.102.0638.

12. Joint_FAO and JECFA (2006). Safety Evaluation of Certain Food Additives (World Health Organization).

13. World Health Organization (2013). Guidelines for Efficacy Testing of Spatial Repellents.

14. Afify, A., Betz, J.F., Riabinina, O., Lahondère, C., and Potter, C.J. (2019). Commonly used insect repellents hide human odors from *Anopheles* mosquitoes. Curr. Biol. *29*, 3669–3680.e5. https://doi.org/10.1016/j.cub.2019.09.007.

15. Melo, N., Capek, M., Arenas, O.M., Afify, A., Yilmaz, A., Potter, C.J., Laminette, P.J., Para, A., Gallio, M., and Stensmyr, M.C. (2021). The irritant receptor TRPA1 mediates the mosquito repellent effect of catnip. Curr. Biol. *31*, 1988–1994.e5. https://doi.org/10.1016/j.cub.2021.02.010.

16. Raji, J.I., Melo, N., Castillo, J.S., Gonzalez, S., Saldana, V., Stensmyr, M.C., and DeGennaro, M. (2019). *Aedes aegypti* mosquitoes detect acidic volatiles found in human odor using the IR8a pathway. Curr. Biol. *29*, 1253–1262.e7. https://doi.org/10.1016/j.cub.2019.02.045.

17. Larsson, M.C., Domingos, A.I., Jones, W.D., Chiappe, M.E., Amrein, H., and Vosshall, L.B. (2004). Or83b encodes a broadly expressed odorant receptor essential for *Drosophila* olfaction. Neuron *43*, 703–714. https://doi.org/10.1016/j.neuron.2004.08.019.

18. Degennaro, M., McBride, C.S., Seeholzer, L., Nakagawa, T., Dennis, E.J., Goldman, C., Jasinskiene, N., James, A.A., and Vosshall, L.B. (2013). Orco mutant mosquitoes lose strong preference for humans and are not repelled by volatile DEET. Nature *498*, 487–491. https://doi.org/10.1038/nature12206.

19. Majeed, S., Hill, S.R., Birgersson, G., and Ignell, R. (2016). Detection and perception of generic host volatiles by mosquitoes modulate host preference: context dependence of (R)-1-octen-3-ol. R. Soc. Open Sci. *3*, 160467. https://doi.org/10.1098/rsos.160467.

20. De Obaldia, M.E., Morita, T., Dedmon, L.C., Boehmler, D.J., Jiang, C.S., Zeledon, E.V., Cross, J.R., and Vosshall, L.B. (2022). Differential mosquito attraction to humans is associated with skin-derived carboxylic acid levels. Cell *185*, 4099–4116.e13. https://doi.org/10.1016/j.cell.2022.09.034.

21. Benton, R., Vannice, K.S., Gomez-Diaz, C., and Vosshall, L.B. (2009). Variant ionotropic glutamate receptors as chemosensory receptors in *Drosophila*. Cell *136*, 149–162. https://doi.org/10.1016/j.cell.2008.12.001.

22. Task, D., Lin, C.-C., Vulpe, A., Afify, A., Ballou, S., Brbic, M., Schlegel, P., Raji, J., Jefferis, G.S.X.E., Li, H., et al. (2022). Chemoreceptor co-expression in *Drosophila melanogaster* olfactory neurons. eLife *11*, e72599. https://doi.org/10.7554/eLife.72599.

23. Herre, M., Goldman, O.V., Lu, T.-C., Caballero-Vidal, G., Qi, Y., Gilbert, Z.N., Gong, Z., Morita, T., Rahiel, S., Ghaninia, M., et al. (2022). Non-canonical odor coding in the mosquito. Cell *185*, 3104–3123.e28. https://doi.org/10.1016/j.cell.2022.07.024.

24. Adavi, E.D., Dos Anjos, V.L., Kotb, S., Metz, H.C., Tian, D., Zhao, Z., Zung, J.L., Rose, N.H., and McBride, C.S. (2024). Olfactory receptor coexpression and co-option in the dengue mosquito. Preprint at bioRxiv *q*, q. https://doi.org/10.1101/2024.08.21.608847.

25. Pullmann-Lindsley, H., Huff, R.M., Boyi, J., and Pitts, R.J. (2024). Odorant receptors for floral- and plant-derived volatiles in the yellow fever mosquito, *Aedes aegypti* (Diptera: Culicidae). PLoS One *19*, e0302496. https://doi.org/10.1371/journal.pone.0302496.

26. Zeng, F., Xu, P., and Leal, W.S. (2019). Odorant receptors from *Culex quinquefasciatus* and *Aedes aegypti* sensitive to floral compounds. Insect Biochem. Mol. Biol. *113*, 103213. https://doi.org/10.1016/j.ibmb.2019.103213.

27. Andreazza, F., Valbon, W.R., Wang, Q., Liu, F., Xu, P., Bandason, E., Chen, M., Wu, S., Smith, L.B., Scott, J.G., et al. (2021). Sodium channel activation underlies transfluthrin repellency in *Aedes aegypti*. PLoS Negl. Trop. Dis. *15*, e0009546. https://doi.org/10.1371/journal.pntd.0009546.

28. Liu, F., Wang, Q., Xu, P., Andreazza, F., Valbon, W.R., Bandason, E., Chen, M., Yan, R., Feng, B., Smith, L.B., et al. (2021). A dual-target molecular mechanism of pyrethrum repellency against mosquitoes. Nat. Commun. *12*, 2553. https://doi.org/10.1038/s41467-021-22847-0.

29. Pereira, T.D., Tabris, N., Matsliah, A., Turner, D.M., Li, J., Ravindranath, S., Papadoyannis, E.S., Normand, E., Deutsch, D.S., Wang, Z.Y., et al. (2022). SLEAP: A deep learning system for multi-animal pose tracking. Nat. Methods *19*, 486–495. https://doi.org/10.1038/s41592-022-01426-1.

30. Matthews, B.J., McBride, C.S., Degennaro, M., Despo, O., and Vosshall, L.B. (2016). The neurotranscriptome of the *Aedes aegypti* mosquito. BMC Genomics *17*, 32. https://doi.org/10.1186/s12864-015-2239-0.

31. Dennis, E.J., Goldman, O.V., and Vosshall, L.B. (2019). *Aedes aegypti* mosquitoes use their legs to sense DEET on contact. Curr. Biol. *29*, 1551–1556.e5. https://doi.org/10.1016/j.cub.2019.04.004.

32. Hol, F.J., Lambrechts, L., and Prakash, M. (2020). BiteOscope, an open platform to study mosquito biting behavior. eLife *9*, e56829. https://doi.org/10.7554/eLife.56829.

33. Bandell, M., Story, G.M., Hwang, S.W., Viswanath, V., Eid, S.R., Petrus, M.J., Earley, T.J., and Patapoutian, A. (2004). Noxious cold ion channel TRPA1 is activated by pungent compounds and bradykinin. Neuron *41*, 849–857. https://doi.org/10.1016/S0896-6273(04)00150-3.

34. Corfas, R.A., and Vosshall, L.B. (2015). The cation channel TRPA1 tunes mosquito thermotaxis to host temperatures. eLife *4*, e11750. https://doi.org/10.7554/eLife.11750.

35. Kwon, Y., Kim, S.H., Ronderos, D.S., Lee, Y., Akitake, B., Woodward, O.M., Guggino, W.B., Smith, D.P., and Montell, C. (2010). *Drosophila* TRPA1 channel is required to avoid the naturally occurring insect repellent citronellal. Curr. Biol. *20*, 1672–1678. https://doi.org/10.1016/j.cub.2010.08.016.

36. Vulpe, A., and Menuz, K. (2021). Ir76b is a co-receptor for amine responses in *Drosophila* olfactory neurons. Front. Cell. Neurosci. *15*, 759238. https://doi.org/10.3389/fncel.2021.759238.

37. Ye, Z., Liu, F., Sun, H., Ferguson, S.T., Baker, A., Ochieng, S.A., and Zwiebel, L.J. (2022). Discrete roles of Ir76b ionotropic coreceptor impact olfaction, blood feeding, and mating in the malaria vector mosquito *Anopheles coluzzii*. Proc. Natl. Acad. Sci. USA *119*, e2112385119. https://doi.org/10.1073/pnas.2112385119.

38. Enjin, A., Zaharieva, E.E., Frank, D.D., Mansourian, S., Suh, G.S.B., Gallio, M., and Stensmyr, M.C. (2016). Humidity sensing in *Drosophila*. Curr. Biol. *26*, 1352–1358. https://doi.org/10.1016/j.cub.2016.03.049.

39. Hussain, A., Zhang, M., Üçpunar, H.K., Svensson, T., Quillery, E., Gompel, N., Ignell, R., and Grunwald Kadow, I.C. (2016). Ionotropic chemosensory receptors mediate the taste and smell of polyamines. PLoS Biol. *14*, e1002454. https://doi.org/10.1371/journal.pbio.1002454.

40. Knecht, Z.A., Silbering, A.F., Ni, L., Klein, M., Budelli, G., Bell, R., Abuin, L., Ferrer, A.J., Samuel, A.D., Benton, R., and Garrity, P.A. (2016). Distinct combinations of variant ionotropic glutamate receptors mediate thermosensation and hygrosensation in *Drosophila*. eLife *5*, e17879. https://doi.org/10.7554/eLife.17879.

41. Ni, L., Klein, M., Svec, K.V., Budelli, G., Chang, E.C., Ferrer, A.J., Benton, R., Samuel, A.D.T., and Garrity, P.A. (2016). The ionotropic receptors IR21a and IR25a mediate cool sensing in *Drosophila*. eLife *5*, e13254. https://doi.org/10.7554/eLife.13254.

42. Silbering, A.F., Rytz, R., Grosjean, Y., Abuin, L., Ramdya, P., Jefferis, G.S.X.E., and Benton, R. (2011). Complementary function and integrated wiring of the evolutionarily distinct *Drosophila* olfactory subsystems.

J. Neurosci. *31*, 13357–13375. https://doi.org/10.1523/JNEUROSCI.2360-11.2011.

43. Lee, Y., Poudel, S., Kim, Y., Thakur, D., and Montell, C. (2018). Calcium taste avoidance in *Drosophila*. Neuron *97*, 67–74.e4. https://doi.org/10.1016/j.neuron.2017.11.038.
44. Matthews, B.J., Dudchenko, O., Kingan, S.B., Koren, S., Antoshechkin, I., Crawford, J.E., Glassford, W.J., Herre, M., Redmond, S.N., Rose, N.H., et al. (2018). Improved reference genome of *Aedes aegypti* informs arbovirus vector control. Nature *563*, 501–507. https://doi.org/10.1038/s41586-018-0692-z.
45. Tracey, W.D., Wilson, R.I., Laurent, G., and Benzer, S. (2003). Painless, a *Drosophila* gene essential for nociception. Cell *113*, 261–273. https://doi.org/10.1016/S0092-8674(03)00272-1.
46. Al-Anzi, B., Tracey, W.D., and Benzer, S. (2006). Response of *Drosophila* to wasabi is mediated by painless, the fly homolog of mammalian TRPA1/ANKTM1. Curr. Biol. *16*, 1034–1040. https://doi.org/10.1016/j.cub.2006.04.002.
47. WHO (2022). Standard Operating Procedure for Testing Insecticide Susceptibility of Adult Mosquitoes in WHO Tube Tests.
48. Norris, E.J., Chen, R., Li, Z., Geldenhuys, W., Bloomquist, J.R., and Swale, D.R. (2022). Mode of action and toxicological effects of the sesquiterpenoid, nootkatone, in insects. Pestic. Biochem. Physiol. *183*, 105085. https://doi.org/10.1016/j.pestbp.2022.105085.
49. McAllister, J.C., and Adams, M.F. (2010). Mode of action for natural products isolated from essential oils of two trees is different from available mosquito adulticides. J. Med. Entomol. *47*, 1123–1126. https://doi.org/10.1603/ME10098.
50. Ffrench-Constant, R.H., Mortlock, D.P., Shaffer, C.D., MacIntyre, R.J., and Roush, R.T. (1991). Molecular cloning and transformation of cyclodiene resistance in *Drosophila*: an invertebrate gamma-aminobutyric acid subtype A receptor locus. Proc. Natl. Acad. Sci. USA *88*, 7209–7213. https://doi.org/10.1073/pnas.88.16.7209.
51. Priestley, C.M., Williamson, E.M., Wafford, K.A., and Sattelle, D.B. (2003). Thymol, a constituent of thyme essential oil, is a positive allosteric modulator of human GABA(A) receptors and a homo-oligomeric GABA receptor from *Drosophila melanogaster*. Br. J. Pharmacol. *140*, 1363–1372. https://doi.org/10.1038/sj.bjp.0705542.
52. Hosie, A.M., Buckingham, S.D., Presnail, J.K., and Sattelle, D.B. (2001). Alternative splicing of a *Drosophila* GABA receptor subunit gene identifies determinants of agonist potency. Neuroscience *102*, 709–714. https://doi.org/10.1016/s0306-4522(00)00483-8.
53. Buckingham, S.D., Biggin, P.C., Sattelle, B.M., Brown, L.A., and Sattelle, D.B. (2005). Insect GABA receptors: splicing, editing, and targeting by antiparasitics and insecticides. Mol. Pharmacol. *68*, 942–951. https://doi.org/10.1124/mol.105.015313.
54. Jones, A.K., Buckingham, S.D., Papadaki, M., Yokota, M., Sattelle, B.M., Matsuda, K., and Sattelle, D.B. (2009). Splice-variant-and stage-specific RNA editing of the *Drosophila* GABA receptor modulates agonist potency. J. Neurosci. *29*, 4287–4292. https://doi.org/10.1523/JNEUROSCI.5251-08.2009.
55. Taylor-Wells, J., Senan, A., Bermudez, I., and Jones, A.K. (2018). Species specific RNA A-to-I editing of mosquito RDL modulates GABA potency and influences agonistic, potentiating and antagonistic actions of ivermectin. Insect Biochem. Mol. Biol. *93*, 1–11. https://doi.org/10.1016/j.ibmb.2017.12.001.
56. Du, Y., Nomura, Y., Satar, G., Hu, Z., Nauen, R., He, S.Y., Zhorov, B.S., and Dong, K. (2013). Molecular evidence for dual pyrethroid-receptor sites on a mosquito sodium channel. Proc. Natl. Acad. Sci. USA *110*, 11785–11790. https://doi.org/10.1073/pnas.1305118110.
57. Grieco, J.P., Achee, N.L., Sardelis, M.R., Chauhan, K.R., and Roberts, D.R. (2005). A novel high-throughput screening system to evaluate the behavioral response of adult mosquitoes to chemicals. J. Am. Mosq. Control Assoc. *21*, 404–411. https://doi.org/10.2987/8756-971x(2006)21[404:Anhsst]2.0.Co;2.
58. Salgado, V.L. (2016). Antagonist pharmacology of desensitizing and non-desensitizing nicotinic acetylcholine receptors in cockroach neurons. Neurotoxicology *56*, 188–195. https://doi.org/10.1016/j.neuro.2016.08.003.
59. Tan, J., Liu, Z., Tsai, T.D., Valles, S.M., Goldin, A.L., and Dong, K. (2002). Novel sodium channel gene mutations in *Blattella germanica* reduce the sensitivity of expressed channels to deltamethrin. Insect Biochem. Mol. Biol. *32*, 445–454. https://doi.org/10.1016/S0965-1748(01)00122-9.

STAR★METHODS

KEY RESOURCES TABLE

REAGENT or RESOURCE	SOURCE	IDENTIFIER
Bacterial and virus strains		
Escherichia coli – Top10 Competent cells, genotype: F⁻*mcr*A Δ(*mrr-hsd*RMS-*mcr*BC) ϕ80*lac*ZΔM15 Δ*lac*X74 recA1 *ara*D139 Δ(*ara-leu*) 7697 galU galK λ–rpsL(Str^R) endA1 nupG	ThermoFisher Scientific, USA	Cat#C404010
Biological samples		
Sheep blood	Håtuna AB, Bro, Sweden	Cat#336; https://www.hatunalab.com
Chemicals, peptides, and recombinant proteins		
Nootkatone FG ≥98%	Sigma-Aldrich	74437; CAS: 4674-50-4
Nootkatone ≥96%	Evolva	N/A
Acetone ACS ≥99,5%	Sigma-Aldrich	179124; CAS: 67-64-1
N,N-diethyl-m-toluamide ≥95% (DEET)	Sigma-Aldrich	36542; CAS: 134-62-3
1-Octen-3-ol ≥98%	Sigma-Aldrich	W280518; CAS:3391-86-4
DMSO ACS ≥99,9%	Sigma-Aldrich	276855; CAS: 67-68-5
n-Heptane ≥99%	Sigma-Aldrich	34873; CAS: 142-82-5
Ethanol ≥99.5%	Fisher Scientific	16651932; CAS: 64-17-5
Ethanol 70%	Fisher Scientific	BP82011; CAS: 64-17-5
CO_2	Linde AG	CAS: 124-38-9
Collagenase B	Sigma-Aldrich	Cat#COLLB-RO
Sodium Chloride	Sigma-Aldrich	S7653; CAS: 7647-14-5
Potassium Chloride	Sigma-Aldrich	P5405; CAS: 7447-40-7
Magnesium Chloride hexahydrate	Sigma-Aldrich	M2393; CAS: 7791-18-6
Calcium Chloride dihydrate	Sigma-Aldrich a	C7902; CAS: 10035-04-8
HEPES	Sigma-Aldrich	H4034; CAS: 7365-45-9
Sodium pyruvate	Sigma-Aldrich	P5280; CAS: 113-24-6
Theophylline	Sigma-Aldrich	T1633; CAS: 58-55-9
Gentamicin sulfate salt	Sigma-Aldrich	G1264; CAS: 1405-41-0
Agar	Promega	Cat#V3841; CAS: 9012-36-6
Phenol	Sigma-Aldrich	P4557; CAS: 108-95-2
Critical commercial assays		
mMESSAGE mMACHINE™ T7 Transcription Kit	ThermoFisher Scientific, USA	Cat# AM1344
NotI Restriction enzyme	New England Biolabs, USA	Cat#R3189L
ApaLI Restriction enzyme	New England Biolabs, USA	Cat#R0507L
BamHI Restriction enzyme	New England Biolabs, USA	Cat#R3136L
BstEII Restriction enzyme	New England Biolabs, USA	Cat#R3162L
TRIzol™-Reagent kit	ThermoFisher Scientific, USA	Cat#15596026
Turbo DNA-free™ kit	ThermoFisher Scientific, USA	Cat#AM1907
RNeasy Mini Kit (50)	QIAGEN N.V., Germany	Cat#74104
SuperScript™ III First-Strand Synthesis System	ThermoFisher Scientific, USA	Cat#18080051
Monarch gel extraction kit	New England Biolabs, USA	Cat#T1020L
T4 DNA ligase	ThermoFisher Scientific, USA	Cat#15224041
6X gel loading dye	New England Biolabs, USA	Cat#B7025S
E.Z.N.A Plasmid DNA Mini Kit I	Omega Bio-tek, Inc., USA	Cat#D6943-02
Deposited data		
Ae. aegypti Rdl clone	This paper	GenBank: PQ497334

(*Continued on next page*)

Continued		
REAGENT or RESOURCE	SOURCE	IDENTIFIER
Experimental models: Cell lines		
Xenopus laevis ovary	Xenopus1, USA	https://xenopus1.com
Experimental models: Organisms/strains		
Ae. aegypti/Orlando^{wt}	DeGennaro Lab, Florida International University, Miami, USA	N/A
Ae. aegypti/Liverpool^{wt}	Vosshall lab, The Rockefeller University, New-York, USA	N/A
Ae. aegypti/$^{Orco5/16}$	DeGennaro Lab, Florida International University, Miami, USA	N/A
Ae. aegypti/Ir8a$^{Attp/Dsred}$	DeGennaro Lab, Florida International University, Miami, USA	N/A
Ae. aegypti/TRPA1$^{ECFP-1/ECFP-2}$	Vosshall lab, The Rockefeller University, New-York, USA	N/A
Cx. Quinquefasciatus/Thai^{wt}	Ignell lab, Swedish University of Agricultural Sciences, Sweden	N/A
An. gambiae/G3^{wt}	Ignell lab, Swedish University of Agricultural Sciences, Sweden	N/A
Ae. aegypti/Ir25a$^{19/BamHI}$	Vosshall lab, The Rockefeller University, New-York, USA	N/A
Ae. aegypti/Ir76b$^{32/65}$	Vosshall lab, The Rockefeller University, New-York, USA	N/A
Ae. aegypti/Rockefeller	Ke Dong Lab, Duke University, Durham, USA	N/A
Oligonucleotides		
Primer for PCR-Cloning – AaRdl_Forward: CGCGGATCC*GCCACC*ATGGCGCT GGAAATCGAAGTGCC	This paper	N/A
Primer for PCR-Cloning – AaRdl_Reverse: CGCGGTAACCTTACTTCTCCTCT CCGAGTAGGACC	This paper	N/A
Recombinant DNA		
AaRdl1-1 in pGH19	This paper	N/A
AaNa$_v$1-1 in pGH19	Du et al.[56]	N/A
Software and algorithms		
Python version 3.10.9	Python Software Foundation	https://www.python.org
EAG software 2.2	Ockenfels Syntech GmbH, Germany	https://www.ockenfels-syntech.com
Social LEAP Estimates Animal Pose v1.3.3	SLEAP Developers	https://sleap.ai
Clampex v.10.7 software	Molecular Devices	https://www.moleculardevices.com
OriginPro 2022b	OriginLab Cor, USA	https://www.originlab.com
Other		
Tetramin® fish food	Tetra, Arken Zoo	Cat#16110
Bugdorm Cages (30x30x30)	BugDorm Store	Cat#DP1000B; https://shop.bugdorm.com
Bugdorm Cages (15x15x15)	BugDorm Store	Cat#BD4S1515; https://shop.bugdorm.com
Artificial blood feeder	HemotekTM, UK	Cat#SP6W1-3; http://hemotek.co.uk
Spatial repellency setup	Custom-made	N/A
Whatman Filter Paper	Sigma-Aldrich	Cat#1001500
CO2 flowmeter	Scantec Nordic, Sweden	80.PMR1-017993
Air flowmeter	Scantec Nordic, Sweden	80.PMR1-012793
Photonic Fence Monitoring Device (PFMD)	GH Labs, WA, USA	https://photonicsentry.com
Fork-shaped electrode	Ockenfels Syntech GmbH, Germany	https://www.ockenfels-syntech.com
Signal acquisition	Ockenfels Syntech GmbH, Germany	IDAC-2; https://www.ockenfels-syntech.com

(*Continued on next page*)

Continued

REAGENT or RESOURCE	SOURCE	IDENTIFIER
Pulse generator	Ockenfels Syntech GmbH, Germany	https://www.ockenfels-syntech.com
Basler ace Classic	Basler AG	Basler acA2040-90um; https://www.baslerweb.com
Macro len	Canon	Macro EF 100 mm f/2.8L
WHO tube test	Biogents	https://eu.biogents.com/contract-research-who-cone-test/
Nanoject II	Drummond Scientific Co., USA	https://shop.drummondsci.com
Oocyte Clamp 725-C amplifier	Warner Instrument Cor., USA	https://www.warneronline.com
Digidata 1440A	Molecular Devices, USA	https://www.moleculardevices.com
Borosilicate capillary glass	World Precision Instruments Inc., USA	Cat#1B120F-4
P-97 filament pipet puller	Sutter Instrument Co., USA	https://www.sutter.com
Centrifuged model 5810 R	Eppendorf, Germany	https://www.eppendorf.com
3D printer model S3	Ultimaker, Netherlands	https://ultimaker.com
UltiMaker 2.85mm NFC PLA - Black 750g	Ultimaker, Netherlands	https://www.dynamism.com Cat#1609
18-gauge polytetrafluoroethylene	Scientific commodities Inc., USA	Cat#BB311-18
Micromanipulator	Narishige, Japan	U-3C
Valve controller model VC6 with perfusion kit	Warner Instrument Cor., USA	VC6

EXPERIMENTAL MODEL AND STUDY PARTICIPANT DETAILS

Animal rearing

Wild-type *Ae. aegypti* (Orlando and Liverpool strains), *Cx. quinquefasciatus* (Thai strain) and *An. gambiae* (G3 strain) were reared at 27±1 °C, 70±5% RH, and a 12L:12D light cycle. All immature stages were raised in distilled water, with larvae fed Tetramin® fish food (Tetra, Arken Zoo, Sweden). Adults emerged in Bugdorm cages (15 cm x 15 cm x15 cm or 30 cm x 30 cm x 30 cm; MegaView Science, Talchung, Taiwan) and were provided with 10% sucrose solution. All adult females were offered sheep blood (Håtuna AB, Bro, Sweden) from a membrane feeder (HemotekTM, Discovery Workshops, Accrington, UK) 5 days post-emergence for 1 h. The following *Ae. aegypti* heteroallelic lines were utilized: $Orco^{5/16}$, $TRPA1^{ECFP\text{-}1/ECFP\text{-}2}$, $Ir8a^{Attp/Dsred}$, which were generated by crossing their corresponding homozygous mutants and collecting F1 progeny. The heteroallelic mutants $Ir25a^{19/BamHI}$ and $Ir76b^{32/65}$ were generated using the crossing scheme previously described.[20] All *Ae. aegypti* mutants were maintained under the same conditions as wild-type, except for $Ir25a^{19/BamHI}$ and $Ir76b^{32/65}$, which were blood-fed on human arms.

All behavioral experiments were carried out with 5-15 day-old female mosquitoes only fed sucrose solution. All assays were carried out at Zeitgeber time 4 to 11 at the same rearing conditions.

METHOD DETAILS

Chemical reagents

Nootkatone FG ≥98%, acetone ACS ≥99,5%, *N*,*N*-diethyl-*m*-toluamide ≥95% (DEET), 1-octen-3-ol ≥98%, DMSO ACS ≥99,9% and n-heptane ≥99% were obtained from Sigma-Aldrich® (Stockholm, Sweden). We in addition obtained samples of nootkatone from Evolva AG, with ≥96% purity. Ethanol ≥99.5% and 70% were obtained from Fisher Scientific (Lund, Sweden). CO_2. purchased from Linde AG (Sweden).

Mosquito behavior experiments

Spatial repellency assay

A modified spatial repellency assay[57] was used to investigate mosquito avoidance behavior in response to nootkatone or DEET stimuli without direct contact. The plexiglass setup included two treatment cylinders (L: 14 cm, W: 10 cm), one release chamber for mosquitoes (L: 16 cm, W: 10 cm), linking sections, and two metallic drums covered with treated nylons inside the cylinders (L: 13 cm, W: 9 cm). Mosquitoes females were placed in the central chamber and allowed to acclimate for 8 min. 500 μL solution of nootkatone or DEET (1% w/v and 5% w/v) was added to a nylon sock and allowed to dry for 2 min before coating the drums with the nylon and placing them inside the cylinders. Blank controls were run with acetone. The entire system was then covered with an opaque cloth, with viewing ports left uncovered to attract mosquitoes with light at the ends. Mosquitoes were released by opening the doors simultaneously, and their responses to the stimuli were observed over 8 min. Subsequently, the number of mosquitoes in each chamber was counted, and the setup was cleaned with 70% ethanol after each run. 10 mosquitoes of each strain were used for each

experiment and each treatment was subjected to at least 6 replicates. Repellency indices were calculated using the formula: RI = (Nc - Nt) / (Nc + Nt), where Nc represents the number of females in the control chamber and Nt represents the number of females in the treatment chamber. All spatial repellency tests are summarized in Table S1.

Close proximity response assay

Each mosquito was individually transferred to a cage (30 cm x 30 cm x 30 cm BugDorm, Taiwan) and allowed a 5 min acclimation period. A 1000 mL pipette tip, containing a filter paper soaked with the test stimulus, was gently brought near the mosquito. The tip was placed on the cage wall where the mosquito was resting. The mosquito's behavior was observed for 30 s, during which the time to take-off was recorded. Three different odorants were tested: acetone and 30% w/v nootkatone. The order of exposure was randomized, with a 2-min rest period between each exposure (n = 30).

Uniport olfactometer assay

A modified uniport assay[16] was used to evaluate mosquito attraction to human host stimuli. The uniport consists of a plexiglass tube (L: 75 cm, W: 13 cm) attached to a small cylindrical trap (L: 10 cm, W: 5 cm), which houses the mosquitoes before the experiment. At the other end of the plexiglass tube was a hollow box (L: 25 cm, W: 20 cm) connected to the stimulus chamber. CO_2 was released through the stimulus chamber to create an airflow of 1 L/min (80.PMR1-017993, Scantec Nordic, Sweden) towards the release trap. The CO_2 concentration in the assay was maintained at 2500-2700 ppm by a carbon dioxide monitor (Extech CO240, Elfa, Sweden). The humidified airflow was regulated at 9 L/min by an air flowmeter (80.PMR1-012793, Scantec Nordic, Sweden). Mosquitoes were released from the small cylinder trap and allowed to respond to stimuli (human subject hand treated with 500 μL acetone, nootkatone 5% w/v, 10% w/v) for 8 min. 10 female *Ae. aegypti* were used for each experiment and each treatment was subjected to 10 replicates. Mosquitoes were considered attracted if they flew upwind through the uniport into the attraction trap. Mosquitoes that moved out of the cylindrical trap were considered activated. A blank trial with no odor stimulus was run to ensure the cleanliness of the setup.

Short range repellency assay with human scent

We conducted close-range repellency experiments by recording the behavioral response of mosquitoes using the Photonic Fence Monitoring Device (PFMD) (GH Labs, WA, USA) over a period of 2 min. The PFMD was positioned 150 cm away within a Plexiglas cage (30cm x 30cm) with a retroreflective background. Insects were released through a rectangular opening at the bottom (4 cm x 7 cm), which was subsequently covered with a nylon net allowing exposure to the stimulus (human subject's arm treated with either 5% w/v nootkatone or acetone) while preventing direct contact of the insects with the skin. We conducted a total of 9 experimental recordings for each treatment using 3 female *Ae. aegypti* in each replicate. The zip file containing metadata from the recordings was analyzed using the virtual interface of Photonic Sentry (https://www.pfmd.net/), and the raw data files, containing temporal information in the form of datetime and positional information as X, Y, and Z coordinates, were processed using Python 3.10.9 with the pandas, numpy, and matplotlib packages.

Close-up feeding assay

Non-blood-fed females (5-10 d-old) were allowed to come into contact with a volunteer's arm and continue to feed blood through a circular opening (3 cm diameter) at the base of a Plexiglas box (10 cm x 10 cm). The females were acclimatized in the box for 2 min without skin exposure and the experiment began by placing the arm in the opening. The behavior was recorded for 5 or 20 min (20 fps) with a Basler acA2040-90um camera controlled using Pylon 5 software and equipped with a 100 mm macro lens (Canon macro EF 100 mm f/2.8L). The skin was previously treated with 100 μL of acetone as a control treatment or 5% w/v nootkatone. 5 females were used per replicate (n=4-7) for each treatment. The Social LEAP Estimates Animal Pose [SLEAP v1.3.3] software package was used for pose estimation. The trained pose estimation skeleton contained 13 anatomical positions of interest on the mosquito: head, abdomen, end of the stylet, end of the tarsus of the forelegs (L, R), midleg (L, R), hindleg (L, R), end of the femur (L, R) and end of the tibia of the forelegs (L, R). Thorlabs components were used to arrange all optical components and the experimental cage at suitable distance.

WHO insecticide susceptibility test

Insecticide bioassays with 10% w/v and 20% w/v nootkatone were done following the instructions of the World Health Organization.[47] 10 female mosquitoes were aspirated into each one of the five holding tubes, and acclimatization was allowed for 30 min. Control and exposure tubes were prepared, with nootkatone or acetone impregnated filter paper placed in after 5 min of solvent evaporation. Mosquitoes were gently blown into the exposure tubes and set for a 1 h exposure period. Following exposure, mosquitoes were transferred back to holding tubes and provided with a 10% sugar solution. They were kept for 24 h in controlled conditions before assessing mortality. Mosquitoes were classified as dead or knocked down based on immobility or inability to fly.

Electroantennography (EAG)

Wild type and *Orco*$^{5/16}$ female mosquitoes were cold-anesthetized. The distal end of both antennae was placed in the recording electrode a fork-shaped electrode while the base of the mosquito head was placed at the reference electrode. The electrode (Ockenfels Syntech GmbH, Germany) was covered with conducting gel. This electrode was then connected to a high input impedance preamplifier (Syntech, Germany) using Ag/AgCl junctions. EAG responses were digitized using an IDAC-2 signal acquisition system and visualized using a dedicated EAG software (Syntech, Germany). A pulse generator CS-05 (Syntech, Germany) facilitates the stimulation of the antenna with a 2 s pulse, using an analytical airflow of 300 mL/min through a Pasteur pipette containing a filter paper soaked with 10 μL solution of the test compounds (nootkatone, 1-octen-3-ol, and n-heptane, each at 0.0001% w/v). A continuous flow of 500 mL/min of humidified air was maintained during the recordings. 6 to 9 replicates on different individuals of each strain were performed. The raw data files were processed using Python 3.10.9 with pandas, numpy, and plotly.graph_objects packages.

Isolation of an *Aedes aegypti* Rdl full-length cDNA

For cloning a full-length transcript of the Rdl GABA receptor gene, total RNA was extracted from heads of 50 female *Ae. aegypti* (Rockefeller strain) using TRIzol-Reagent kit (Invitrogen™). The total RNA was then treated with Turbo DNA-free kit (Invitrogen™) and further cleaned up using RNeasy kit (Qiagen). Oligo-dT primers were used for the first strand cDNA synthesis using SuperScriptIII kit (Invitrogen™). Based on the Rdl coding sequence (GenBank Accession Number: U28803), the following primers were designed to amplify Rdl cDNA: AaRdl_Forward (CGC**GGATCC***GCCACC*ATG*G*CGCTGGAAATCGAAGTGCC) and AaRdl_Reverse (CGC**GGTAACC**TTACTTCTCCTCTCCGAGTAGGACC). Both primers contained overhangs that included the restriction enzyme cutting sites (bold) for downstream vector cloning. In AaRdl_Forward primer, a Kozak sequence (underlined) was introduced by addition of 6 nucleotides (italicized) before the start codon and a point mutation from T to G on the 4 positions of the coding sequence (italicized). The PCR products were cloned into pGH19, a *Xenopus* oocyte expression vector. First, both the PCR products and the plasmid DNA were digested with the restriction enzymes (BamHI, and BstEII, New England Biolabs) and were then gel-extracted and purified using Monarch gel extraction kit (New England Biolabs). T4 DNA ligase (Promega) was used to complete the insertion of the PCR products into the vector. The ligated plasmids were then transformed into Top10 *E. coli* bacteria line (Invitrogen™) and grown in agar plates as the manufacturer protocols. Candidate colonies were handpicked into liquid LB growth medium and shaken for 18 h for vigorous colony growth. A "quick check" step was performed prior to plasmid isolation to screen for the presence of plasmids of expected size in each bacteria culture. For that, a 50 μL aliquot of the bacterial culture from each candidate tube was mixed with 50 μL of phenol (Sigma-Aldrich) and 10 μL of 6X gel loading dye (New England Biolabs). The mixture was vigorously vortexed and centrifuged at 14,000 rpm for 10 min at 4 °C. Approximately 20 μL of supernatant was loaded and separated in an electrophoresis agar gel and DNA bands of 3-4 kb were screened to select for candidate bacteria culture. Potential candidate culture solutions were further processed for plasmid isolation using E.Z.N.A Plasmid DNA Mini Kit (Omega Bio-tek) and isolated plasmid was sequenced using Oxford Nanopore technologies (Plasmidsaurus). The full-length *Ae. aegypti* Rdl clone was deposited in GenBank under the Accession Number: PQ497334.

Expression of *AaegRdl1-1* and *AaNa$_v$1-1* in *Xenopus* oocytes

Mature stage IV and V *Xenopus* oocytes were isolated from ovaries of the African clawed frog (*Xenopus laevis*) from Xenopus1 (Dexter-MI, USA) for cRNA injection. Briefly, about 4 mL of oocytes clusters obtained by mechanically separating pieces of the ovary tissue, was incubated with 4 mg collagenase (Roche Diagnostics GmbH, Germany) in 11 mL calcium-free ND96 saline containing 96 mM NaCl, 2 mM KCl, 1.8 mM $CaCl_2$, 1 mM $MgCl_2$, 5 mM HEPES, 2.5 mM Na-pyruvate, 0.5 mM theophylline, supplemented with gentamicin at 100 mg/L. Follicle cells and follicle membranes were then removed with forceps. Isolated oocytes were cultured in the ND96 saline. To prepare cRNA for oocyte injection, plasmid DNA of an isolated *Rdl* clone, *AaegRdl1-1* was linearized using *NotI* which does not cut the insert, followed by *in vitro* transcription with T7 polymerase using the mMESSAGE mMACHINE kit (Ambion, Austin, TX). The plasmid DNA containing the *AaNa$_v$1-1* was linearized using ApaL-I, and in vitro transcription was performed as for the *AaegRdl1-1*. As in previous studies,[56] *AaTipE* auxiliary sub-unity was co-injected with *AaNa$_v$1-1* at 1:1 ratio, to achieve robust Na_v expression on the oocytes. The *AaTipE* was linearized with NotI before in vitro transcription as described earlier. In-vitro transcribed capped RNA of *AaegRdl1-1* or *AaNa$_v$1-1:AaTipE* eluted in DEPC-water was injected into oocytes to a dose ranging from 0.5 to 2 ng per cell using a Nanoject II (Drummond Scientific Co. Broomall, PA-USA), set to delivery 27.6 nL of solution per injection in the fast mode.

Two-electrode voltage clamp recordings and data analysis

Electrophysiological recordings were conducted using an Oocyte Clamp 725-C amplifier (Warner Instrument Cor. Hamden, CT-USA), and data were acquired using a Digidata 1440A analog-digital interface and managed with its Clampex v.10.7 software (Molecular Devices, San Jose, Ca-USA). Microelectrodes were made from borosilicate capillary glass (1B120F-4, World Precision Instruments Inc. Sarasota, FL-USA) in a P-97 puller (Sutter Instrument Co. CA), being backfilled with a warm solution of 3 M KCl + 1.5% agar (resistance ranging from 1 to 1.5 MΩ) in Rdl recordings, but 0.5 MΩ for Na_v).

To achieve faster chemical delivery and washout during the recording of GABA-induced currents, we adapted the u-tube delivery system previously developed[58] for isolated cockroach neurons. Briefly, cells were bathed in a custom designed 3D PLA-printed recording chambers, with ND96 recording solution (96 mM NaCl, 2 mM KCl, 1.8 mM $CaCl_2$, 1 mM $MgCl_2$, 10 mM HEPES) from a gravity-fed 18-gauge polytetrafluoroethylene (PTFE) tubing (Scientific commodities Inc., Lake Havasu City, AZ-USA) placed about 2 mm from the oocyte (Figure 4B, left flow line). The ligand (i.e., GABA) solutions were flown inside another gravity/vacuum PTFE tubing (Figure 4B, right flow line). The middle section of this tubing was bent to form a u-shaped loop, on which a small hole was made using a 0.2 mm insect pin, that was placed close to the oocyte using a micromanipulator (Narishige, U-3C, Japan). The flow of both bath and u-tube lines were controlled by two pinch valves (from a VC6 controller, Warner Instrument Cor. Hamden, CT-USA), one interrupting the main bath flow onto the cell, and the other placed downstream from the u-tube loop. When the pinch valves are open, the solution from the U-tube does not flow into the chamber, and the oocyte is continuously washed with fresh bath solution. When the pinch valves are closed (for 5 s), the u-tube solution directly bathes the oocyte, while the bath flow is interrupted. Upon reopening of both valves, ligand application ceases and the strong bath flow immediately wash away the ligand solution from the cell.

U-tube solutions with increasing concentrations of the ligand (i.e., GABA) were applied alone or in continuous presence of 100 μM of nootkatone (both in bath and u-tube solutions) until a maximum response plateau was achieved. For each GABA concentration, the

peak response (amplitude) of three consecutive GABA pulses were averaged. The responses for each GABA concentration were normalized to peak current at the highest GABA concentration in its curve, and data was fit to a Boltzmann regression analysis in OriginPro 2022b (OriginLab Cor. Northampton, MA-USA). Each individual cell (replicate) thus yielded an EC_{50} for GABA in presence and another in absence of nootkatone. These EC_{50} values were used for a Student's *t*-test in SigmaPlot v.15 (Inpixon Inc. Palo Alto, Ca-USA). Additionally, a global curve fit was performed containing all the replicates values, which yield a single EC_{50} value. This overall EC_{50} value was confirmed to be very similar to the average of individual replicate curve fits, but also provided the 95% upper and lower confidence interval bands plotted along with the observed data.

For the recording of $AaNa_v1$-1, oocytes were clamped to -120 mV, and the following protocols were recorded before, and after exchanging the bath recording solution without nootkatone to a nootkatone containing solution. 1) Voltage dependent of activation protocol, from 20 ms step depolarizations ranging from -85 to +65 mV, in 5 mV increments; 2) Voltage dependent of activation protocol, from 20 ms step depolarizations ranging from -85 to +65 mV, in 5 mV increments after a train of 50X 5 ms pre-pulses to +50 mV at 20 Hz, as used in ß-toxins recordings; 3) Tail current from a repolarization to -120 mV after a 20 ms pulse to -10 mV after a train of 100X 5 ms pre-pulses to -10 mV at 66 Hz. The solution exchange was performed by applying 10 mL of freshly prepared solution at one side of the chamber from a 10 mL syringe while a vacuum tube syphon collected the solution on the other side. Incubation with nootkatone in the bath before recording the protocols was 10 min. Conductance data was calculated and normalized to maximum conductance before being fit to a Boltzmann equation as previously described.[59]

QUANTIFCATION AND STATISTICAL ANALYSIS

All statistics were performed using Python 3.10.9 with the pandas, numpy, and scipy.stats packages. Statistical details related to sample size and *p* values are reported in the figure legends.